2021 IEEE International Conference on Environment and Electrical Engineering and 2021 IEEE Industrial and Commercial Power Systems Europe (EEEIC / I&CPS Europe) | 978-1-6654-3613-7/21/$31.00 ©2021 IEEE | DOI: 10.1109/EEEIC/ICPSEurope51590.2021.9584625

Stochastic Distribution Network Operation for Transactive Energy Markets

Erik Erudiel Santos-Gonzalez, Guillermo Gutierrez-Alcaraz
Tecnológico Nacional de México I. T. Morelia
Morelia, Mexico
erudiel.santos@gmail.com, guillermo.ga@morelia.tecnm.mx

Ali Esmaeel Nezhad
School of Energy Systems LUT University
Lappeenranta, Finland
ali.esmaeelnezhad@gmail.com

Mohammad S. Javadi
INESC TEC
Porto, Portugal
msjavadi@gmail.com

Gerardo J. Osório
REMIT/UPT and C-MAST/UBI
Covilhã, Portugal
gjosilva@gmail.com

João P. S. Catalão
FEUP and INESC TEC
Porto, Portugal
catalao@fe.up.pt

***Abstract*—In this paper, a stochastic optimization model is developed for optimal operation of the active distribution networks. The proposed model is investigated on the transactive energy market in the presence of active consumers, local photovoltaic power generations and storage devices. The stochastic behavior of photovoltaic panel power generation units and load consumptions have been modeled using scenario generations and scenario reduction technique. Besides, the stochastic nature of the demand power as well as rooftop photovoltaic panels have been investigated in this paper. In the transactive energy market model, the distribution system operator is the main responsible for the market-clearing mechanisms and controlling the net power exchange between the distribution network and upstream grid. The proposed model is tested and verified on a radial medium voltage distribution network with 16 buses.**

***Keywords*—Demand response, distribution system, electric vehicles, parking lots, photovoltaic generation, transactive market.**

I. Introduction

Operation of the distribution electricity network is one of the main activities of distribution companies (DisCos). The DisCos are the responsible entities in the power systems in both regulated and deregulated paradigm. Serving the end-users' demand, monitoring distribution network, asset management, and maintaining the power quality of electricity are the main roles of DisCos in the power system. The current smart grids benefit from active consumers, local power generations, like photovoltaic (PV) and electrical energy storage (EES) units. In the transactive energy (TE) markets, the distributed energy providers increase the reliability and flexibility of the network operations while reducing the operational costs by reducing the network power losses, shifting the controllable loads to off-peak periods, and strategic energy storing with EES devices [1]. The possibility of the data exchange between the entities in this area improves the interoperability of the mentioned transactive energy market. A considerable share of research works has been carried out in the field of optimal operation of power networks in the presence of local and onsite power generating units, EES devices, and demand response programs [1]-[4].

A framework for the day-ahead (DA) transactive market is proposed in [3]. In this framework, the distribution system operator (DSO) operates a transactive market, and it is responsible for the optimal and secure operation of its local distribution area. A DC power flow formulation is used for network modeling. Thus, distribution losses are neglected.

In [5], the authors extend the previous work by adding a rigorous formulation of the diesel generators (DG) minimum on/off times, ramping, spinning reserve constraints, and distribution losses. Considering distribution losses in the transactive energy problem allows the DSO to achieve superior operational decisions and minimize purchasing power from the market. At the distribution operation level, in addition to conventional feeder relief and protection schemes, the need for new grid services such as phase balancing and grid-edge reactive and voltage support is emerging [6]. Hence, full nonlinear AC power flow equations need to be used to model power losses and reactive power more accurately. A distribution market that determines the real-time value of transactive energy enabling the power consumers of the distribution system to make energy transactions in real-time is proposed in [7].

The microgrid has been introduced to ensure the successful integration of renewable energy sources (RES) with the traditional distribution system [8]. Fitting microgrids in smart distribution networks provide the expected functionalities that improve power delivery's reliability and economy [9]. The transactive energy market concept is applied to a multi-microgrid scenario where each microgrid can trade its energy with neighboring microgrids [10]. Optimal scheduling of the distributed energy resources (DERs) is targeted with microgrids profit maximization under the TE management is reported in [11]. Microgrids can submit the hourly bids/offers in the DA market to specify their energy consumption/production for the next energy exchanging day. A stochastic framework for the energy management of a microgrid to minimize the energy cost from the grid has been developed in [12].

In [13] proposes a two-stage robust stochastic programming model for optimal scheduling of commercial microgrids equipped with 100% RESs. Uncertainty quantifying was carried out by intending the fluctuations of RERs outputs, volatility of energy market price, and stochastic behaviors of consumers. A comprehensive review on the transactive energy market in the microgrids is investigated in [14], addressing architectures, distributed ledger technologies, and detailed market analysis.

This paper presents a holistic model aiming at achieving optimal operation strategy for day-ahead distributing networks. The main contributions of this research are as follows: A TE management framework is proposed for optimal scheduling of DERs and DR in an active distribution networks in the DA market. DSO is responsible for the market-clearing mechanisms and controlling the net power exchange between the distribution network and upstream grid.

Erik Erudiel acknowledges support from CONACyT through a scholarship to pursue graduate studies at Instituto Tecnológico de Morelia (ITM), Programa de Graduados e Investigación en Ingeniería Eléctrica (PGIIE). J.P.S. Catalão acknowledges the support by FEDER funds through COMPETE 2020 and by Portuguese funds through FCT, under POCI-01-0145-FEDER-029803 (02/SAICT/2017). G.J. Osório acknowledges the support by UIDB/00151/2020 research unit (C-MAST) funded by FCT.

978-1-6654-3613-7/21/$31.00 ©2021 IEEE

Uncertainty on photovoltaic panel power generation units and load consumptions are modeled using scenario generations and scenario reduction techniques. The maximum number of charge-discharge cycles during the day is considered to extend battery cycle life. The remainder of the paper is organized as follows. Section II describes the proposed transactive energy model. Numerical results are provided and discussed in Section III. Finally, Section IV draws relevant conclusions and suggests future research.

II. Mathematical Formulation

This section first describes the proposed TE problem formulation in detail. Subsequently, the load and PV uncertainty modeling and scenario reduction technique is presented.

A. Transactive Energy Modeling

The objective function in (1) minimizes the expected production, start-up, shut-down, BESS costs, and the revenue/cost of energy selling/purchasing to/from the distribution network. This problem is subject to generation, system, network, BESS, DR, and electricity exchanging constraints. The mathematical TE model is:

$$Min \sum_{s\in S}\rho_s \sum_{t\in T}\left(\begin{array}{l}\sum_{i\in Ng}\left(C\left(Pg_{i,t,s}\right)+sdc_i z_{i,t,s}+suc_i w_{i,t,s}\right)\\ +\sum_{s\in Ns}\left(c^{Deg}_{s,t}r^c_{s,t}+c^{Dis}_{s,t}r^d_{s,t}\right)-\sum_{n=1}^{Nnp}\pi_t NP_{n,t}\end{array}\right) \tag{1}$$

subject to:

$$P_{i,t,s}\left(V_t,\theta_t\right)+Pd_{i,t,s}+r^c_{i,t,s}=Pg_{i,t,s}+PV_{i,t,s}+r^d_{i,t,s}+NP_{i,t,s} \tag{2}$$

$$Q_{i,t,s}\left(V_t,\theta_t\right)+Qd_{i,t,s}=Qg_{i,t,s} \tag{3}$$

$$\sum_{i\in Ng} Rg^{Up}_{i,t,s}\geq R^{Up}_{req,t} \tag{4}$$

$$\sum_{i\in Ng} Rg^{Down}_{i,t,s}\geq R^{Down}_{req,t} \tag{5}$$

$$u_{i,t,s}Pg^{Min}_i\leq Pg_{i,t,s}\leq u_{i,t,s}Pg^{Max}_i \tag{6}$$

$$u_{i,t,s}Qg^{Min}_i\leq Qg_{i,t,s}\leq u_{i,t,s}Qg^{Max}_i \tag{7}$$

$$0\leq Rg^{Up}_{i,t,s}\leq u_{i,t,s}Pg^{Max}_i-Pg_{i,t,s} \tag{8}$$

$$0\leq Rg^{Down}_{i,t,s}\leq Pg_{i,t,s}-u_{i,t,s}Pg^{Min}_i \tag{9}$$

$$-Pg_{i,t-1,s}+Rg^{Down}_{i,t-1,s}\leq u_{i,t-1,s}RU_i+w_{i,t,s}RSU_i \tag{10}$$

$$-Pg_{i,t,s}+Rg^{Up}_{i,t-1,s}+Pg_{i,t-1,s}+Rg^{Down}_{i,t,s}\leq u_{i,t,s}RD_i+z_{i,t,s}RSI \tag{11}$$

$$u_{i,t,s}=Pg^{on-off}_i \qquad 0\leq t\leq L^{Up,Min}_i+L^{Down,Min}_i \tag{12}$$

$$\sum_{\tau=t-Pg^{UP}_i+1}^{t} w_{i,\tau,s}\leq u_{i,t,s} \qquad t\geq L^{Up,Min}_i \tag{13}$$

$$\sum_{\tau=t-Pg^{Down}_i+1}^{t} z_{i,\tau,s}\leq 1-u_{i,t,s} \qquad t\geq L^{Down,Min}_i \tag{14}$$

$$w_{i,t,s}+z_{i,t,s}\leq 1 \tag{15}$$

$$u_{i,t,s}=u_{i,t-1,s}+w_{i,t,s}-z_{i,t,s} \tag{16}$$

$$u_{i,t,1}=u_{i,t,s} \tag{17}$$

$$P_{ij,t,s}=\left(V^2_{i,t}-V_{i,t}V_{j,t}\cos\left(\theta_{ij,t}\right)\right)G_{ij}-V_{i,t}V_{j,t}B_{ij}\sin\left(\theta_{ij,t}\right) \tag{18}$$

$$Q_{ij,t,s}=-\left(V^2_{i,t}-V_{i,t}V_{j,t}\cos\left(\theta_{ij,t}\right)\right)B_{ij}-V_{i,t}V_{j,t}G_{ij}\sin\left(\theta_{ij,t}\right) \tag{19}$$

$$\sqrt{P^2_{ij,t}+Q^2_{ij,t}}\leq S^{Max}_{ij} \tag{20}$$

$$V^{Min}_i\leq V_{i,t,s}\leq V^{Max}_i \tag{21}$$

$$R^{c,Min}_i u^{BESS}_{i,t,s}\leq r^c_{i,t,s}\leq R^{c,Max}_i u^{BESS}_{i,t,s} \tag{22}$$

$$R^{d,Min}_i u^{BESS}_{i,t,s}\leq r^d_{i,t,s}\leq R^{d,Max}_i u^{BESS}_{i,t,s} \tag{23}$$

$$SOC_{i,t,s}=SOC_{i,t-1,s}+\eta^c_i r^c_{i,t,s}-\frac{r^d_{i,t,s}}{\eta^d_i} \tag{24}$$

$$SOC^{Min}_i\leq SOC_{i,t,s}\leq SOC^{Max}_i \tag{25}$$

$$SOC_{i,0}-SOC_{i,T}=0 \tag{26}$$

$$u^{BESS}_{i,t,s}=u^{BESS}_{i,t-1,s}+y^{BESS}_{i,t,s}-z^{BESS}_{i,t,s} \tag{27}$$

$$\sum_{\tau=t-SOC^{NT}_i+1}^{t} y^{BESS}_{i,\tau,s}\leq u^{BESS}_{i,t,s} \tag{28}$$

$$\sum_{t=1}^{t} y^{BESS}_{i,t,s}\leq SOC^{NC}_i \tag{29}$$

$$u^{BESS}_{i,t,1}=u^{BESS}_{i,t,s} \tag{30}$$

$$NP^{Min}\leq NP_{i,t,s}\leq NP^{Max} \tag{31}$$

$$SL^{Min}_i\leq SL_{i,t,s}\leq SL^{Max}_i \tag{32}$$

$$\sum_{t=1}^{T} SL_{i,t,s}=0 \tag{33}$$

where

$$L^{Up,Min}_i=\left(Pg^{Up}_i-Pg^{Up,init}_i\right)Pg^{on-off}_i$$

$$L^{Down,Min}_i=\left(Pg^{Down}_i-Pg^{Down,init}_i\right)\left(1-Pg^{on-off}_i\right).$$

where $C\left(Pg_i\right)$ is the total diesel generation cost, Pg_i is the output power of the generator i, sdc_i and suc_i are the shut-down/start-up cost of DG *i*, respectively, $c^{Deg}_{i,t}$ and $c^{Dis}_{i,t}$ are the degradation and discharge costs of the BESS *i*, respectively, $PV_{i,t,s}$, $NP_{i,t,s}$, $r^c_{i,t,s}$, $r^d_{i,t,s}$, and $Pd_{i,t,s}$ are active power from solar PV, exchanged power, BESS charging and discharging rates and load demand at bus *i*, respectively, $Qg_{i,t,s}$ and $Qd_{i,t,s}$ are the reactive power from DG *i* and load demand at bus *i*, respectively, Pg^{Max}_i and Pg^{Min}_i are active power limits from DG *i*, Qg^{Max}_i and Qg^{Min}_i are reactive power limits from DG *i*, $Rg^{Down}_{i,t,s}$ and $Rg^{Up}_{i,t,s}$ are ramp shut-down/start-up limits from DG *i*, $R^{Down}_{req,t}$ and $R^{Up}_{req,t}$ are, RD_i and RU_i are ramp-down/up rates from DG *i*, RDU_i and RSU_i are ramp shut-down/start-up limits from DG *i*, $u_{i,t}$, $w_{i,t}$, and $z_{i,t}$ binary variables, $P_{ij,t,s}$ and $Q_{ij,t,s}$ are active and reactive power flows in the line connecting buses *i-j*, respectively, B_{ij} and G_{ij} are the susceptance and conductance of line connecting buses *i-j*, respectively, $V_{i,t}$ is the voltage magnitude of bus *i*, V^{Max}_i and V^{Min}_i are the maximum and minimum voltage magnitude limits of bus *i*, $\theta_{ij,t}$ is the phase angle difference in the line connecting buses *i-j*, $S^{Max}_{ij,t}$ is the maximum apparent power flow in the line connecting buses *i-j*, $SOC_{i,t,s}$ is the energy storage level at bus *i*, $r^c_{i,t,s}$ and $r^d_{i,t,s}$ are, respectively, $R^{c,Max}_i$ and $R^{d,Max}_i$ are the charge and discharge upper bounds, respectively, $R^{c,Min}_i$ and $R^{d,Min}_i$ are the charge and discharge lower bounds, respectively, η^c_n and η^d_n are the charge and discharge efficiencies, respectively, SOC^{Max}_i and SOC^{Min}_i are the limits of state of charge, SOC^{NC}_i is the maximum number of load cycles, $u^{BESS}_{i,t,s}$, $y^{BESS}_{i,t,s}$ and $z^{BESS}_{i,t,s}$ are binary variables,

NP^{Min} and NP^{Max} are the exchanged power limits, $SL_{i,t,s}$ is the shifted load power, and SL_i^{Max} and SL_i^{Min} are the shiftable load limits. $L_i^{Down,Min}$ and $L_i^{Up,Min}$ are the number of periods unit *i* must be initially offline/online due to its minimum down/up time constraint, $Pg_i^{Down,init}$ and $Pg_i^{Up,init}$ are the number of periods unit *i* has been offline/online, respectively, prior to the first period of the time span, Pg_i^{Down} and Pg_i^{Up} are the minimum down and up times of unit *i*, respectively, and Pg_i^{on-off} is the initial commitment state of unit *i*.

Constraints (2)–(3) represent the bus active and reactive power balance, respectively. Constraints (4) and (5) are system reserve requirements. Constraints (6)-(11) define that the generated power, ramp-up, and ramp-down rates should be within limits. Constraints (12)-(14) represent the minimum up/down times. Constraints (15) and (16) preserve the logic of running, start-up, and shut-down status changes. (17) represents the non-anticipativity generation scheduling constraint. Constraints (18) and (19) are power flows in the lines. Constraints (20) and (21) represent the limitations of complex power and voltage magnitude, respectively. Constraints (22) and (23) represent the charging/discharging operational bounds of BESS, respectively. Equation (24) models the energy balance of BESS. The SOC limit is stated by (25). Constraint (26) indicates that the SOC at the end of the scheduling period would be the same as that at the beginning of period. Constraints (27)-(30) preserve the state of charge's logic and the maximum number of charging/discharging cycles, respectively. Constraint (31) represents electricity exchanging constraints. Constraint (32) represents load shifted limits and constraint (33) indicates that adjustable loads are shifted to other allowable periods.

B. Load and PV Uncertainty Modeling and Scenario Reduction Technique

Different uncertain parameters can adversely impact the operation of an active distribution network, e.g. the load demand as well as solar power generation by the PV panel. Among the available effective techniques to characterize the uncertainties, the scenario-based optimization approach has captured attention as an efficient method with the capability of accommodating probable scenarios. In this respect, the roulette wheel mechanism and lattice Monte-Carlo simulation are deployed in this paper to provide the decision maker with the required initial scenarios to start off solving the problem. However, it should be noted that the more the number of generated scenarios, the more precise the characterization will be obtained at the end. Hence, a relatively large number of scenarios are typically needed to properly model the behavior of an uncertain parameter. This number of scenarios would impose a huge computational load to the problem, which in some cases causes the intractability of the problem. Thus, an efficacious method should be applied to alleviate the computational burden of the initial scenarios by appropriately and accurately mitigating the number of scenarios to a rational number. Accordingly, the first step is to generate the initial number of scenarios by using the lattice Monte-Carlo simulation. First, a random value should be randomly generated in the interval {0, 1} and assigned to every uncertain parameter. Unlike the original Monte-Carlo simulation, using the uniform distribution, the lattice Monte-Carlo simulation deploying the N-Point lattice rule of rank r in dimension d would be implemented as [2], [3]:

$$\sum_{p}^{r} \frac{k_p}{n_p}\left(\sum_{u}^{U} v_u\right) \bmod 1,\ k_p = 1,....,U;\ j = 1,...,r \tag{34}$$

It is noteworthy that v_u shows the vectors associate with dimension *d* derived by utilizing the Monte-Carlo simulation. The number of random values in every scenario is expressed by dimension *d*. Any of the lattice Monte-Carlo simulation scenario comprises a vector associated with dimension *d* of the random values mapped on the interval {0, 1} formed by utilizing a set of values k_p. It is worth mentioning that the lattice Monte-Carlo simulation better and more uniformly characterizes the uncertain parameter compared to the Monte-Carlo simulation. It is also noteworthy that the uncertainty of the load and solar power generation would be characterized by using the error specified by the probability distribution function. In this regard, a continuous probability distribution function would be discretized to be used for the modeling the load demand and solar power generation [4]. The detailed procedure is available in [3].

The probability distribution function is mapped on the zero mean and the distribution function is discretized to several intervals, each with the width equal to the standard deviation and a specific probability value [15]. Accordingly, with respect to each interval and its associated probability, the roulette wheel mechanism would be used for scenario generation. The probabilities, associated with each interval should also be normalized such that their aggregate value is equal to 1. Furthermore, as any of the intervals holds an accumulated value of the normalized probability, every scenario, generated by this technique includes a binary parameter vector showing the solar power generation and load demand at any of the time slots of the operation period. As mentioned before, the uncertain parameter would be more accurately described by a large number of scenarios, which in turn causes a huge computational load. As a result, an effective scenario reduction method should be used to make a trade-off between the accuracy and the computational burden. In this relation, this paper employs the backward scenario reduction method as mentioned in [2], [3] to alleviate the number of primarily generated scenarios, highly relying upon the preciseness needed for the problem.

III. Numerical Examples

The proposed approach is tested with the IEEE 16-bus radial distribution system [16]. Fig. 1 shows the IEEE 16-bus distribution system single line diagram. The simulations were carried out on a PC with an Intel Core i5, 2.40-GHz, 8 GB RAM, and 64-bit Windows 10 PRO using DICOPT solver under GAMS [17]. For this case study, DICOPT was run with default parameters; the relative optimality gap tolerance was kept at 0.0001. It is assumed that 20% of the forecasted load is shiftable.

Fig. 2 and Fig. 3 show the hourly PV generation and hourly demand profile, respectively, over a 24-hour horizon. The total demand is proportionally divided by each load bus. 10 scenarios in the cases of solar PV and load demand are considered. Each scenario has a probability of ρ_s = 1/10.

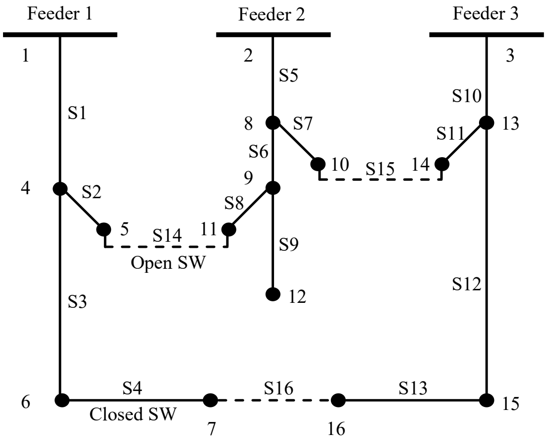

Fig. 1. IEEE 16-node distribution network.

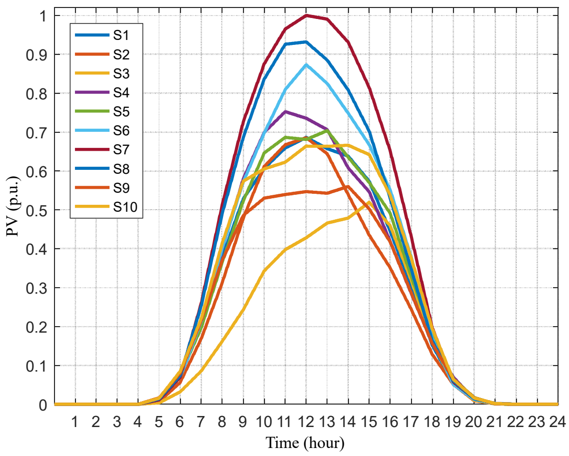

Fig. 2. Hourly PV generation pattern [19].

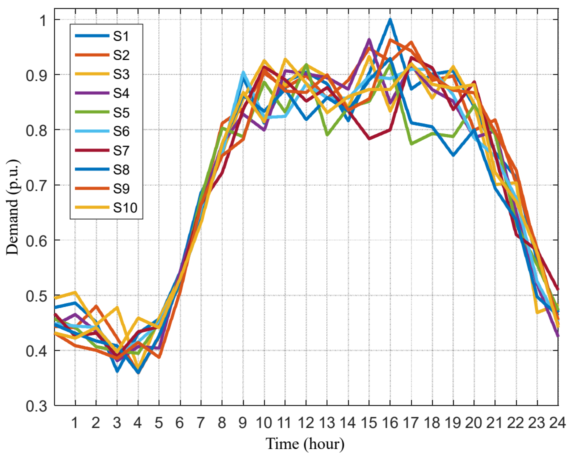

Fig. 3. Hourly demand level in p.u. of the system peak [19].

We use the backward scenario reduction method to obtain 10 groupings of the scenarios of PV and demand from the 1000 scenarios produced by the lattice Monte-Carlo simulation [18]. For reproducibility purposes, system data can be downloaded from [19].

To investigate the proposed model's effectiveness, two wholesale electricity market price cases are considered at the exchange point. The hourly electricity prices depicted in Fig. 4 are from California Independent System Operator (CAISO) of days February 6, 2019, and March 02, 2020. It can be observed that in Case 1, the electricity market price is much higher than in Case 2.

Three DGs are connected in buses 7, 12, and 15, respectively. Three PV systems (0.70 MW) are connect in buses 9, 12, and 14. Three BESSs are connected in buses 2, 5, and 10. Discharging and degradation costs of BESSs are set at 0.02 and 5, respectively. The unit's DG and BESS data are shown in Table I and Table II, respectively. DG costs are taken from [20] and scaled-down. The maximum number of charge-discharge cycles is set to 1.

Table III shows the on/off DG optimal solution. The differences in the start-up and shut-down for the generating units are in bold. DG 3 was operating all the time in both scenarios since it has the lowest production cost.

In case 1, during periods 17 to 24, DG2 is in service, and energy is exported. Although the price is high during periods 6 to 9, there is no energy exported because other constraints (i.e., reserves, ramps, and minimum times) prevent taking advantage of the high prices. After period 9, power cannot be imported, even when the price decreases substantially, due to previous operational constraints, which makes it challenging to reduce the output power of the DG.

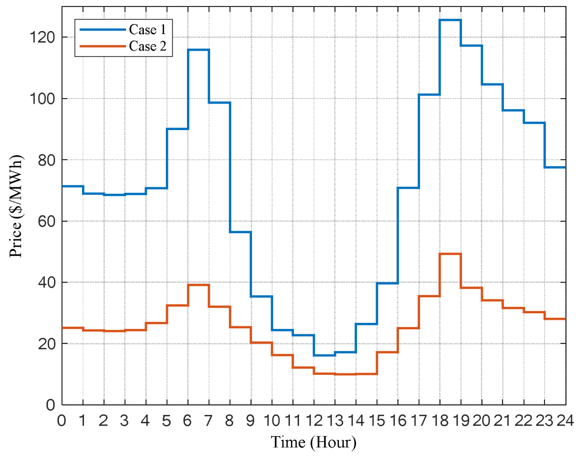

Fig. 4. Hourly electricity price at a wholesale market for the two cases.

TABLE I. PARAMETERS OF DIESEL GENERATORS

DG	RU_i MWh	RD_i MWh	RSD_i MWh	RSU_i MWh	Pg_i^{Min} (MW)	Pg_i^{Max} (MW)	Qg_i^{Min} (MVA)	Qg_i^{Max} (MVA)
1	1	1	1	1	1	4.12	-4.026	4.026
2	1	1	1	1	1	3.53	-3.3065	3.3065
3	1	1	1	1	1	4.83	-4.4715	4.4715

TABLE II. PARAMETERS OF BESS

	Cap_m	SOC_m^{Min}	DP_m^{Max}	RP_m^{Max}	η_m^{BESS}
1	1.5	0.3	0.5	0.5	0.94
2	1.5	0.3	0.5	0.5	0.94
3	2	0.2	0.4	0.4	0.94

TABLE III. ON/OFF STATUES OF DIESEL GENERATORS

DG	1	2	3	4	5	6	7	8	9	10	11	12	13	14	15	16	17	18	19	20	21	22	23	24
Case 1																								
1	0	0	0	0	0	0	0	0	0	0	0	0	0	1	1	1	1	1	1	1	1	1	1	1
2	0	0	0	0	0	0	0	0	0	0	0	0	0	0	0	0	1	1	1	1	1	1	1	1
3	1	1	1	1	1	1	1	1	1	1	1	1	1	1	1	1	1	1	1	1	1	1	1	1
Case 2																								
1	0	0	0	0	0	0	0	0	0	0	0	0	0	1	1	1	1	1	1	1	1	1	1	1
2	0	0	0	0	0	0	0	0	0	0	0	0	0	0	0	0	**0**	**0**	**0**	**0**	**0**	**0**	**0**	**0**
3	1	1	1	1	1	1	1	1	1	1	1	1	1	1	1	1	1	1	1	1	1	1	1	1

DR seeks to eliminate the maximum peak of demand. This allows increasing the demand in periods of minimum demand for later periods of maximum demand, flattening the demand profile, but the total consumption remains unchanged.

Charge and discharge optimal statues of BESS are reported in Table IV and V, respectively. As can be seen, BESS charged in off-peak and discharged in peak hours.

The voltage profile is shown in Fig. 5. The voltage limits are considered as 0.95 p. u. and 1.05 p. u. It can be seen that the median of the voltage profile is similar in both cases. However, in case 1, there is a higher spread, which means that the voltage presents a more significant fluctuation compared to case 2.

Voltage density over the time horizon is depicted in Fig. 6. A similar voltage profile and deviation for both cases are observed during the first 13 hours. After hour 13, for case 1, there is an increase in voltage magnitude, resulting from the increase in generation for export purposes, since the generators also provide reactive power. On the other hand, there is an import in case two, which means a greater flow from the power system, increasing the voltage drop, and a decrease in the DG units' generation power.

TABLE IV. CHARGE STATUES OF BESS

	1	2	3	4	5	6	7	8	9	10	11	12	13	14	15	16	17	18	19	20	21	22	23	24
Case 1																								
1	0	0	1	0	0	0	0	0	0	0	0	1	1	1	0	0	0	0	0	0	0	0	0	1
2	0	0	1	1	0	0	0	0	0	0	0	1	1	1	0	0	0	0	0	0	0	0	0	1
3	0	0	1	0	0	0	0	0	0	0	1	1	1	1	1	0	0	0	0	0	0	0	0	0
Case 2																								
1	0	0	0	0	0	0	0	0	0	0	0	0	1	1	1	0	0	0	0	0	0	0	0	0
2	0	0	0	0	0	0	0	0	0	0	0	0	1	1	1	0	0	0	0	0	0	0	0	0
3	0	0	0	0	0	0	0	0	0	0	0	1	1	1	1	0	0	0	0	0	0	0	0	0

TABLE V. DISCHARGE STATUES OF BESS

	1	2	3	4	5	6	7	8	9	10	11	12	13	14	15	16	17	18	19	20	21	22	23	24
Case 1																								
1	0	0	0	0	0	0	1	1	0	0	0	0	0	0	0	0	0	0	1	1	0	0	0	0
2	0	0	0	0	0	0	1	1	0	0	0	0	0	0	0	0	0	0	1	1	1	0	0	0
3	0	0	0	0	0	0	1	1	0	0	0	0	0	0	0	0	0	1	1	1	1	0	0	0
Case 2																								
1	0	0	0	0	0	1	1	0	0	0	0	0	0	0	0	0	0	0	1	0	0	0	0	0
2	0	0	0	0	0	0	1	0	0	0	0	0	0	0	0	0	0	0	1	1	0	0	0	0
3	0	0	0	0	0	0	1	0	0	0	0	0	0	0	0	0	0	1	1	1	0	0	0	0

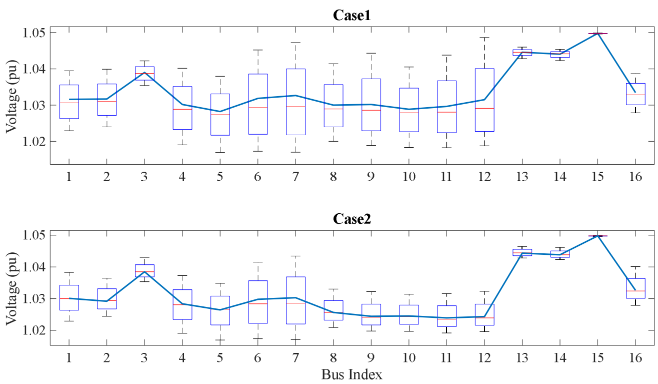

Fig. 5. Voltage profile for both cases.

The average real power distribution locational marginal prices (DLMPs) for the two cases are reported in Fig. 7. As can be seen, the DLMPs are highly influenced by the LMP at the exchange bus. When the LMP at the exchange bus is higher than the corresponding DLMP, local onsite DG units in the distribution network increase their power generation to export. In each case, the DLMPs are similar because there is no congestion in the system. The difference between the DLMP of each bus is due to the distribution losses, which in essence, are small.

Table VI shows the total expected costs for the two cases. As can be observed, the lowest expected cost is achieved in Case 1 because the market price at the delivery point is much lower concerning Case 1; hence no energy is exported.

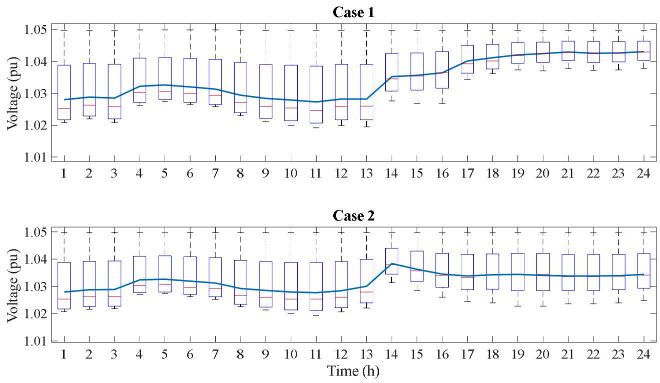

Fig. 6. Hourly voltage profile for both cases.

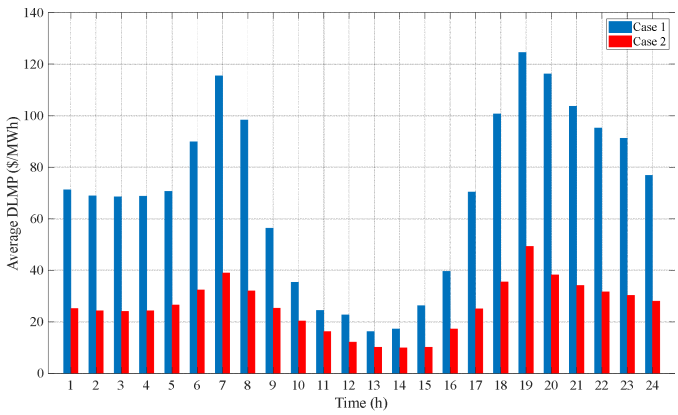

Fig. 7. DLMP for both cases.

TABLE VI. TOTAL EXPECTED COSTS

Case	1	2
Costs ($)	49,061.1999	64,537.2177

IV. CONCLUSION

This paper presented a stochastic transactive energy model considering uncertainties of solar PV generation and load demand. The resulting model is cast as an instance of mixed-integer nonlinear programming. The proposed model was analyzed through numerical studies on a 16-bus distribution system. Results show that the proposed model can assist DSOs to optimally schedule local DERs and power interchanges with the bulk system for the day-ahead market. We suggest that future research should use a linearized AC power flow to reduce the computational burden.

REFERENCES

[1] A. Adeyemi, M. Yan, M. Shahidehpour, S. Bahramirad, and A. Paaso, "Transactive energy markets for managing energy exchanges in power distribution systems," *The Electricity Journal*, Vol. 33, no. 9, Nov. 2020, 106868.

[2] M. S. H. Nizami, M. J. Hossain, B. M. R. Amin, M. Kashif, E. Fernandez, and K. Mahmud, "Transactive energy trading of residential prosumers using battery energy storage systems," in 2019 IEEE Milan PowerTech, PowerTech 2019, 2019.

[3] Y. K. Renani, M. Ehsan, and M. Shahidehpour, "Optimal transactive market operations with distribution system operators," *IEEE Trans. Smart Grid*, vol. 9, no. 6, pp. 6692–6701, Nov. 2018

[4] M. Lotfi, C. Monteiro, M. S. Javadi, M. Shafie-Khah, and J. P. S. Catalao, "Optimal prosumer scheduling in transactive energy networks based on energy value signals," in SEST 2019 - 2nd International Conference on Smart Energy Systems and Technologies, 2019, pp. 1–6.

[5] Erik Erudiel Santos-Gonzalez and Guillermo Gutierrez-Alcaraz, "Day-ahead transactive market operations with smart distribution power systems," 52nd North American Power Symposium.

[6] F. Rahimi and A. Ipakchi, "Using a transactive energy framework," *IEEE Electrification Magazine*, Dec. 2016.

[7] M. Ghamkhari, "Transactive energy pricing in power distribution systems," 2019 IEEE Green Technologies Conference (GreenTech), Apr. 2019.

[8] X. Lu, S. Bahramirad, J. Wang, and ChenChen, "Bronzeville community microgrids: A reliable, resilient and sustainable solution for integrated energy management with distribution systems," *The Electricity Journal*, vol. 28, no. 10, pp. 29-42, Dec. 2015.

[9] M. E. Khodayar, S. D. Manshadi, and A. Vafamehr, "The short-term operation of microgrids in a transactive energy architecture," *The Electricity Journal*, vol. 29, no. 10, pp. 41–48, Dec. 2016.

[10] H. S. V. S. Kumar Nunna, and D. Srinivasan, "Multi-agent based transactive energy framework for distribution systems with smart microgrids," *IEEE Trans. on Industrial Informatics*, vol. 13, no. 5, pp. 2241 – 2250, Oct. 2017.

[11] M Daneshvar, B. Mohammadi-ivatloo, S. Asadi, M. Abapour, and A. Anvari-Moghaddam, "A transactive energy management framework for regional network of microgrids," 2019 International Conference on Smart Energy Systems and Technologies (SEST), Sep. 2019.

[12] D. Prudhviraj, P. B. S. Kiran, and N. M. Pindoriya, "Stochastic energy management of microgrid with nodal pricing," *Journal of Modern Power Systems and Clean Energy*, vol. 8, no. 1, pp. 102–110, Jan. 2020.

[13] M. Daneshvar, B. Mohammadi-ivatloo, K. Zare, and S. Asadi, "Two-stage robust stochastic model scheduling for transactive energy based renewable microgrids," *IEEE Trans. on Industrial Informatics*, vol. 16, no. 11, pp. 6857 – 6867, Nov. 2020.

[14] M. F. Zia, M. Benbouzid, E. Elbouchikhi, S. M. Muyeen, K. Techato, and J. M. Guerrero, "Microgrid transactive energy: review, architectures, distributed ledger technologies, and market analysis," *IEEE Access*, vol. 8, pp. 19410–19432, Jan. 2020.

[15] M. S. Javadi, A. Anvari-Moghaddam, J. M. Guerrero, A. E. Nezhad, M. Lotfi, and J. P. S. Catalão, "Optimal operation of an energy hub in the presence of uncertainties," in *2019 IEEE International Conference on Environment and Electrical Engineering and 2019 IEEE Industrial and Commercial Power Systems Europe (EEEIC / I&CPS Europe)*, Jun. 2019.

[16] S. Civanlar, J. J. Grainger, H. Yin, and S. S. H. Lee, "Distribution feeder reconfiguration for loss reduction," *IEEE Trans. Power Delivery*, vol. 3, no. 3, pp. 1217–1223, July 1988.

[17] "GAMS." [Online]. Available: https://www.gams.com/

[18] M. S. Javadi, M. Lotfi, A. E. Nezhad, A. Anvari-Moghaddam, J. M. Guerrero, and J. P. S. Catalão, "Optimal operation of energy hubs considering uncertainties and different time resolutions," IEEE Transactions on Industry Applications, vol. 56, no. 5, pp. 5543–5552, Sep.-Oct. 2020.

[19] https://www.dropbox.com/sh/41jdxy997ryqbrw/AADpxyCA3ujKv-7F8W1x6ApXa?dl=0

[20] H. Farzin, M. Fotuhi-Firuzabad, and M. Moeini-Aghtaie, "Stochastic energy management of microgrids during unscheduled islanding period," *IEEE Trans. on Industrial Informatics*, vol. 13, no. 3, pp. 1079-1087, Jun. 2017.